Proc. Natl. Acad. Sci. USA
Vol. 88, pp. 9355–9359, October 1991
Biochemistry

Differential flexibilities in three branches of an N-linked triantennary glycopeptide

(resonance energy transfer/oligosaccharides)

PENGGUANG WU, KEVIN G. RICE*, L. BRAND†, AND Y. C. LEE

Department of Biology, The Johns Hopkins University, Baltimore, MD 21218

Communicated by Saul Roseman, July 22, 1991

ABSTRACT **The solution conformation behavior of complex oligosaccharides was studied by resonance energy transfer, as measured by the time-resolved fluorescence method, to determine the conformational heterogeneity of a triantennary glycopeptide at various temperatures. Groups that acted as a fluorescence donor (naphthyl-2-acetyl, Nap) or acceptor (dansylethylenediamine, Dan) were selectively attached to the N terminus of the peptide and a Gal residue [either 6′ (shown below), 6, or 8] of the oligosaccharide, respectively.**

(6′) Dan-Galβ4GlcNAcβ2Manα6↘
Manβ4GlcNAcβ4GlcNAcβ-Asn-Ala-NH-Nap
(6) Galβ4GlcNAcβ2Manα3↗
(8) Galβ4GlcNAcβ4↗

Time-resolved fluorescence energy-transfer measurements revealed two populations of conformers when Dan was attached to either Gal-6′ or Gal-6. One conformer contained the antenna folded back toward the core region, and a second was in an extended conformation. The two conformations differed in donor–acceptor distance by about 10 Å. Systematically increasing the temperature from 0°C to 40°C increased the ratio of extended to folded forms 2-fold for the Gal-6 isomer and 4-fold for the Gal-6′ isomer, whereas the Gal-8 isomer showed only a single distance population throughout this temperature range. From these data, ΔH and ΔS for the reversible conformational change were calculated to be 3.1 kcal/mol and 10.8 cal/(mol·K) for the Gal-6 isomer and 7.1 kcal/mol and 25.8 cal/(mol·K) for the Gal-6′ isomer. In addition to the structural microheterogeneity commonly associated with glycoproteins, the differential flexibilities of the different branches in the oligosaccharides contribute conformational heterogeneity and should be considered in conformational analysis. The data are discussed in terms of the most probable linkages that contribute to the observed flexibility of the individual triantennary branches, and the biological significance of flexible linkages in complex carbohydrates is considered.

The carbohydrates in glycoproteins are important in maintaining protein stability, in protecting the protein from proteolysis, and in targeting proteins by binding to endogenous lectins (1, 2). Various physical methods have been used to characterize solution conformations of complex glycopeptides or oligosaccharides. From these studies, models have been proposed to account for solution behaviors of certain glycans (3). For example, an umbrella model was suggested based on the radius of gyration of a glycoprotein from small-angle neutron scattering (4). T-shaped or Y-shaped models of N-linked oligosaccharides were proposed according to small-angle x-ray diffraction data (5). Implicit in these models were flexibilities in one or more branches of the oligosaccharides. However, the low resolution in these diffraction techniques precluded a more detailed assignment of the flexible linkages. Similarly, spin-labeled glycopeptides (6) showed interactions between labels on neighboring branches, implying the existence of flexibility; however, the exact site of flexibility could not be located. Proton NMR has been employed to elucidate solution conformations of many sugar linkages (7–9). Results accumulated thus far have demonstrated that the Manα6Man linkage is flexible, whereas Manβ4GlcNAc or Galβ4GlcNAc linkages are more rigid. The flexibility of GlcNAcβ2Man and Manα3Man linkages is less certain (3, 7, 10). NMR measurements of the Manα3Man linkage indicate that it is relatively rigid (7), while results from energy minimization calculations show that it is flexible (10). However, theoretical calculations generally do not account for solvent conditions, which have been shown to be important in the conformations of linkages by molecular dynamics (11). In addition, the solution conformation of certain disaccharides may depend on the environment when incorporated into an oligosaccharide.

Energy-transfer measurements using time-resolved fluorescence have been used to recover distance distributions between two chromophores attached to distant sites along polymer chains, as pioneered by Haas *et al.* (12). In a previous study (13), we applied the fluorescence energy-transfer method to determine distance distribution(s) within a triantennary glycopeptide. The glycopeptide contains a naphthyl-2-acetyl (Nap) group attached to the N terminus of the Ala-Asn peptide as a fluorescence donor and a dansylethylenediamine (Dan) group coupled to a Gal residue (either 6, 6′, or 8) as the acceptor. A single extended distance population was found to separate the donor from the acceptor on Gal-8. Extended and folded distance populations were found to separate the donor from the acceptor either on Gal-6 or on Gal-6′. These results indicate that the linkages in the Gal-8 isomer are relatively rigid and some of those in Gal-6 and -6′ isomers are flexible. We assigned the site of flexibility in the Gal-6 isomer to the GlcNAcβ2Man linkage. By analogy, the same linkage is assumed to be flexible in the Gal-6′ isomer, which in addition contains Manα6Man; thus there are two potential flexible sites in this isomer.

Here we wish to address the question of energetics or temperature dependence of the flexibilities in each isomer. This can be done using time-resolved fluorescence energy-transfer measurements because this method is capable of recovering both the shape of the distance distribution and the relative concentration of each population. The types of linkages in this glycopeptide include those most commonly encountered in N-linked complex carbohydrates (14). Thus

The publication costs of this article were defrayed in part by page charge payment. This article must therefore be hereby marked "*advertisement*" in accordance with 18 U.S.C. §1734 solely to indicate this fact.

Abbreviations: Dan, dansylethylenediamine; Nap, naphthyl-2-acetyl.

*Present address: Department of Pharmaceutics and Pharmaceutical Chemistry, College of Pharmacy, Ohio State University, Columbus, OH 43210-1291.
†To whom reprint requests should be addressed.

the rigidity/flexibility of the linkages found here should be generally applicable to other N-linked glycopeptides.

MATERIALS AND METHODS

The preparation and characterization of the labeled triantennary glycopeptides have been described (15, 16). The fluorescence donor, Nap, attached to the N terminus of the glycopeptide was used to obtain donor lifetimes and quantum yield (13). A Dan group attached to either Gal-6, -6′, or -8 served as the acceptor. The three glycopeptide isomers with donor and acceptor are termed GP-6-DanNap, GP-6′-DanNap, and GP-8-DanNap (13). These modified glycopeptides show comparable (nanomolar) or slightly reduced affinity for binding to the asialoglycoprotein receptor of rat hepatocytes as compared with the unmodified triantennary glycopeptides (13).

Time-resolved fluorescence measurements were performed on a picosecond dye laser pumped by a mode-locked yttrium/aluminum-garnet laser (Spectra-Physics 3000 series). Dye laser output at 580 nm was frequency-doubled to 290 nm to excite the donor. The fluorescence emission was detected at 350 nm with a single-photon-counting apparatus (17). With the addition of a Hamamatsu R1564U-06 microchannel plate photomultiplier tube as a detector, the overall instrument response was about 70 ps. A scattering Ludox solution was used to collect the instrument response. Duplicate or triplicate fluorescence data were collected at each temperature.

The details of the data analysis have been described (13). Here we give only a brief description. The analysis at each temperature involved two steps. In the first step, we analyzed the fluorescence decay of donor alone in the glycopeptide by a sum of exponentials,

$$I_D(t) = \sum \alpha_i \exp(-t/\tau_i), \qquad [1]$$

where α_i and τ_i are the amplitude and lifetime of the ith component. The large number of data points (typically more than 500) from each single-photon-counting measurement permits the judgment of quality of data fit beyond the simple χ^2 statistics commonly used. Correlations among data points can also be examined in detail. We used reduced χ^2, weighted residuals, and autocorrelations of the residuals to judge the fit of Eq. 1 to experimental data.

In the second step, we analyzed the donor decay of the donor–acceptor pair in the glycopeptides by using distance distribution(s) according to

$$I_{DA}(t) = \sum a_k \int P_k(r) \sum \alpha_i \exp\left\{ -\frac{t}{\tau_i}\left[1 + \left(\frac{R_0}{r}\right)^6\right]\right\} dr, \qquad [2]$$

where the first summation refers to the number of distance populations, a_k is the relative concentration of one distribution of distances, $P_k(r)$ defines the shape of one distribution, and the integral covers all donor–acceptor distances over which energy transfer occurs. Each population is normalized to 1. We used the Lorentzian form of $P_k(r)$,

$$P_k(r) = \frac{2}{\sigma_k \pi \left[1 + \left(\frac{r - \bar{r}_k}{\sigma_k}\right)^2\right]}, \qquad [3]$$

where $\bar{r}_k$ is the average distance of the population and σ_k is related to the full width at half maximum height (FWHM) by FWHM = $2\sigma_k$. Because of the narrow width of distribution found for these glycopeptides (13), the exact shape is not very important. However, the choice of this particular distance-distribution form does not in any regard alter our conclusions about the flexibilities of the three branches of the glycopeptide.

We used the known amplitude (α_i) and lifetime (τ_i) of donor decay in the absence of acceptors obtained from Eq. 1 as the input to fit the data with Eq. 2 to determine the distance distribution(s) and the relative concentration(s). The goodness of the fit was judged exactly as in the case of donor-only decay. The reduced χ^2 of all data sets (over 40) ranged from 0.96 to 1.20 for good fit. The Förster distance (R_0) was calculated as described (13) and was scaled with changing quantum yield at each temperature.

RESULTS

Temperature Dependence of Donor Decay for Each Isomer Is Distinct. Fig. 1 shows the fluorescence decays of donor alone and donor in the three donor–acceptor pairs (GP-8-DanNap, GP-6-DanNap, and GP-6′-DanNap) at 0°C and 40°C. The decay of the donor itself increases slightly at higher temperature, probably due to increased thermal deactivation of its excited state. The decay of GP-8-DanNap at 40°C is faster than that at 0°C, but it resembles the shape of the decay at 0°C. In contrast, the decays of GP-6-DanNap and GP-6′-DanNap show crossover at different temperatures. Examination of the early part of the decays in Fig. 1 *C* and *D* (lower channel numbers) revealed slower decay of the donor at higher temperature despite an increased thermal quenching of the donor alone, as in Fig. 1*A*. This can only be achieved by reduction in acceptor quenching at higher temperature. Since GP-8-DanNap does not show crossover as in Fig. 1*B*, the changes in decays of the other two isomers indicate structural changes as a function of temperature. We show later that these changes are due to transition from the folded form to the extended form.

GP-8-DanNap Has One Distance Population Whereas GP-6-DanNap and GP-6′-DanNap Have Two Distance Populations in the 0°–40°C Temperature Range. To obtain more quantitative data, we analyzed the decay curves at all temperatures. The decay of donor alone could be described by a sum of two exponentials. At 20°C, one component has a lifetime of about 27 ns with 94% of the total amplitude. The second component has a lifetime of 2–4 ns. The amplitude of the minor component varies from 4% to 8% in the temperature range used. Since the first component contributes about 99% of the detected signal, it basically defines the shape of the decay. The contribution from the second component is very small.

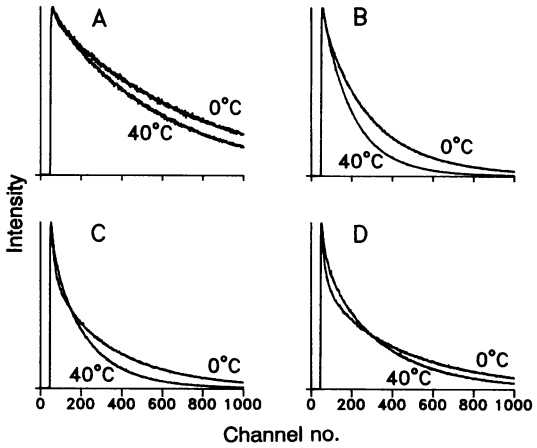

FIG. 1. Fluorescence decays of donor alone (*A*) and donor–acceptor pairs in GP-8-DanNap (*B*), GP-6′-DanNap (*C*), and GP-6-DanNap (*D*) at 0°C and 40°C. Excitation was at 290 nm and emission at 350 nm. Each channel corresponds to 0.042 ns.

Nonetheless we included both components in the data analysis of energy-transfer measurements.

The decay of GP-8-DanNap was analyzed by one population of distances at all temperatures. The results at 30°C are shown in Fig. 2*A* and the fits at other temperatures are similar. Clearly one population fit is adequate for this isomer as judged from the randomness of the weighted residuals and the autocorrelation of the residuals.

Analysis of the decay of GP-6-DanNap with one distance population resulted in a very poor fit (Fig. 2*B*). As we have discussed earlier (13), the fit cannot be improved to a satisfactory degree by choosing an alternative unimodal distance-distribution function or by skewing one distance distribution. A satisfactory fit is obtained when a double distance distribution is used, resulting in the two populations separated by about 10 Å. Similarly the decay of GP-6'-DanNap cannot be fitted with one population (similar to Fig. 2*B*), while a two-population fit gives very good results (similar to Fig. 2*A*).

Temperature Dependence of Each Isomer Is Different. Each of the glycopeptide isomers displays a distinctive temperature dependence of distance distribution(s). For GP-8-DanNap the donor–acceptor distance is not very sensitive to temperature in the range 0–40°C (Fig. 3). The slight shift to shorter distance at higher temperature and the narrowing of the distribution width are probably due to some increased local diffusion of the linker arms of donor and acceptor. The average distance is shortened by <2 Å, which indicates no large-scale interchromophore diffusion or large deformation of the branch occurring within the temperature range. As demonstrated previously (13), the tail of the distribution is due to the modeling procedure. Thus it appears that there is no folded population observable for GP-8-DanNap, suggesting that the Manα3Man linkage in the core region is not sensitive to temperature perturbation.

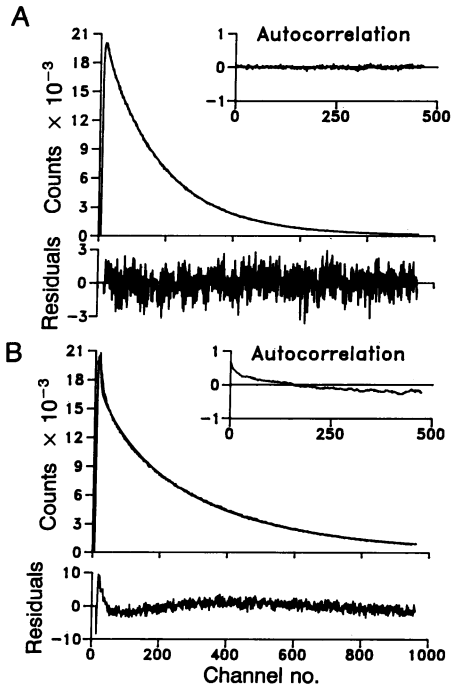

FIG. 2. (*A*) Measured and fitted fluorescence decays of GP-8-DanNap at 30°C. The two curves are indistinguishable. The weighted residuals are shown below the curves. The autocorrelation of the residuals is also shown (*Inset*). (*B*) One distance population fit to the decay of GP-6-DanNap at 30°C. Both the weighted residuals and autocorrelation function show systematic deviation between the fit and measured data.

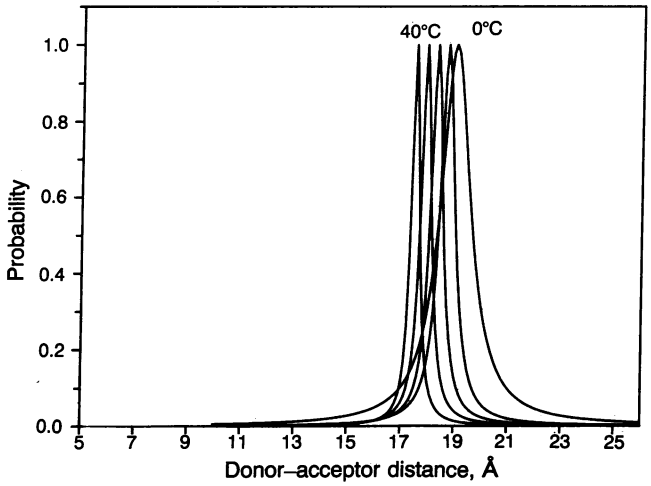

FIG. 3. Distance distribution of GP-8-DanNap at various temperatures. The fit at each temperature was obtained by a Lorentzian distance distribution.

Two distance populations were required to fit the donor decay of GP-6-DanNap between 0°C and 40°C. Fig. 4 shows the change of relative concentration of each distance population. At lower temperature, the folded form is larger than the extended form. As temperature increases, the populations gradually shift to the extended form. At 40°C, the extended form is about twice as abundant as the folded form. We also measured the distance distributions after the sample was cooled down to room temperature, and we got back the same two distance populations. Thus the conversion between the folded and the extended form is reversible and can be regarded as an equilibrium. Since we can obtain the relative concentration of each population (Eq. 2), we are able to extract thermodynamic parameters that govern the conversion. If the equilibrium constant K is defined as the ratio of the extended form to the folded form, then the enthalpy ΔH and entropy ΔS can be obtained (Fig. 5). The enthalpy associated with the conversion of GP-6-DanNap from the folded to the extended form is 3.1 kcal/mol and the entropy is 10.8 cal/(mol·K).

The temperature dependence of GP-6'-DanNap is similar to that of GP-6-DanNap (Fig. 6). At 0°C, the folded form dominates the equilibrium and at 40°C the extended form

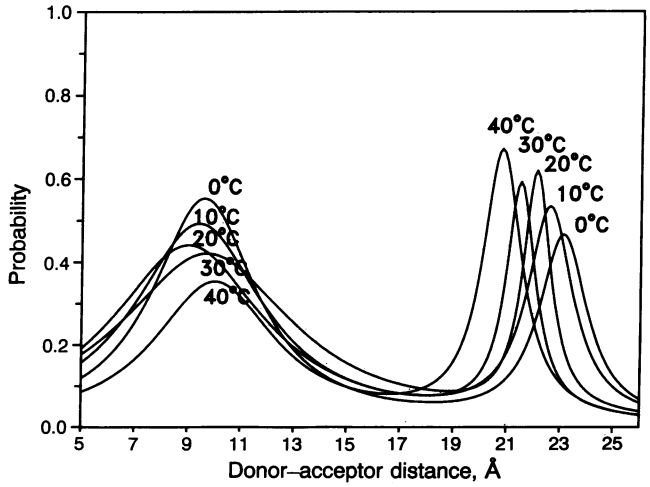

FIG. 4. Distance distribution of GP-6-DanNap at various temperatures. Two distance populations were used to fit the data. The data were plotted to show the relative concentrations of each population by the peak at each temperature and for the same population (extended or folded) at different temperatures.

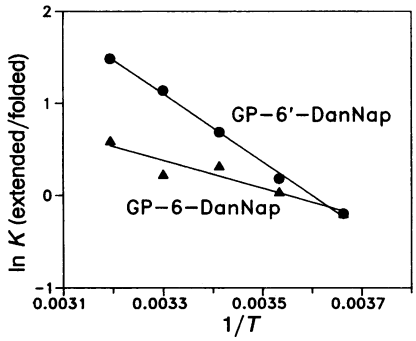

FIG. 5. Temperature dependence of conversion equilibrium constant from folded form to extended form for GP-6-DanNap (▲) and GP-6'-DanNap (●).

dominates over the folded form at a ratio of 4:1, which is twice that observed for GP-6-DanNap in the same temperature range. The conversion likewise is reversible, allowing the calculation of the thermodynamic parameters for unfolding this isomer, which gave ΔH of 7.1 kcal/mol and ΔS of 25.8 cal/(mol·K).

The separation distance determined for the extended form is determined quite accurately, since its average distance is comparable with the Föster distance (R_0) of the donor–acceptor pair used. The folded form is determined with less accuracy due to the large quenching of the donor at shorter donor–acceptor distance and the presence of the extended form. The exact shape of the folded form should be regarded as a rough estimate. Nonetheless, the qualitative features of GP-6-DanNap are such that the folded form remains at about the same separation distance (Fig. 4), while in GP-6'-DanNap it appears that the average separation distance of the folded form increases slightly as the temperature is raised.

DISCUSSION

Differential Flexibilities of the Three Isomers. By time-resolved fluorescence energy-transfer measurements we found that there is only one distance population in GP-8-DanNap and there are two distance populations in GP-6-DanNap and GP-6'-DanNap. A single distance population in GP-8-DanNap indicates that the glycosidic linkages that separate the donor from the acceptor in this glycopeptide isomer are essentially rigid as far as large folded-back deformations are concerned. These include the Galβ4GlcNAc, Manβ4GlcNAc, and GlcNAcβ4GlcNAc linkages, which are already known to be rigid, and the linkage Manα3Man. In the temperature range studied (0–40°C), we found only one distance population, suggesting that the latter linkage is also rigid enough to sustain some thermal fluctuations to be in one conformation (or one cluster of conformations) instead of in multiple conformations. Although this linkage may potentially lead to a folded structure, there seem to be some restrictions for this to occur. The rotation about Manα3Man may, to some degree, be viewed as motion in a cone, which may change inter-Gal distances but not the Gal to N-terminal distance. Preliminary work shows that once the Gal-6, GlcNAc-5, Gal-6', GlcNAc-6', and Man-4' residues are removed, the separation distance between the donor and the acceptor can still be described by one population. The distribution is slightly broader, probably reflecting the fact that there is less steric hindrance for rotation in this straight-chain analogue.

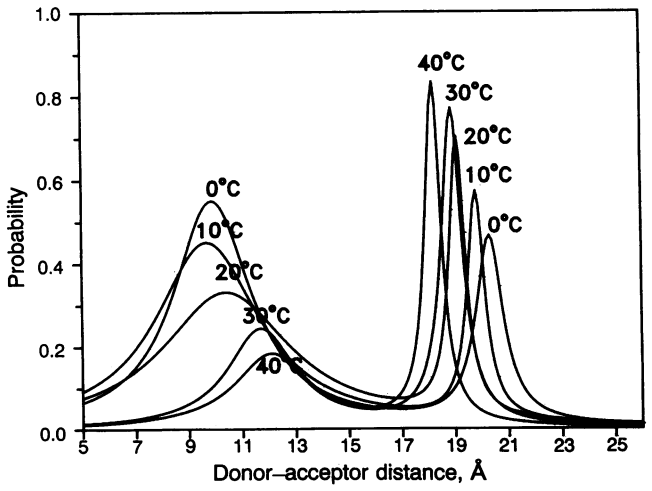

FIG. 6. Distance distribution of GP-6'-DanNap at various temperatures. Two distance populations were used to fit the data. The data were plotted to show the relative concentrations of each population by the peak at each temperature and for the same population (extended or folded) at different temperatures.

The appearance of two distance populations in both GP-6-DanNap and GP-6'-DanNap between 0°C and 40°C suggests that flexible glycosidic linkage(s) exist in these two branches. In a previous study (13), we assigned the GlcNAcβ2Man linkage as the site of flexibility by comparing GP-6-DanNap with GP-8-DanNap, since this is the only distinct linkage in the two isomers. As a result, there are two potential flexible sites in GP-6'-DanNap. By varying the solution temperature in the present study, we have obtained strong evidence that the appearance of two distance populations in GP-6'-DanNap is indeed due to two flexible linkages.

The temperature dependence of population interconversion in GP-6'-DanNap is twice as high as that in GP-6-DanNap (Fig. 5). This is expected if there are two flexible sites, since it is more difficult in terms of energetics to convert from the folded form to the extended form. The positive entropy is consistent with the notion that the folded form is more compact. Clearly the free energy of conversion at all temperatures is very small, so that as solution conditions change, the concentration of each population may shift. Although the free energy of conversion between folded and extended forms is small for both GP-6-DanNap and GP-6'-DanNap, this does not mean that there is a continuum of uniform distance distributions between the two forms. As we pointed out earlier (13), the intermediate distances should be much easier to detect than the folded distance(s). Clearly, the conversion kinetics are not controlled by random diffusion, which would predict apparent higher folded forms at higher temperature. It is likely that the bulky size of the sugars results in a quite high potential barrier for the conversion, thus slowing down the kinetics on the time scale of fluorescence measurements.

The folded and extended structures in complex carbohydrates can explain in more detail some of the earlier observations. The change from one conformation to another can change interterminal distance by about 10 Å. Gervais and Gallot (5) observed two types of lamellar structures in an amphipathic liposaccharide system: T shape and Y shape of the N-linked carbohydrates. The change from T to Y shape resulted in an increase of layer thickness of about 20 Å with two layers of liposaccharides composing one layer of lamellar structure. This is consistent with a change from folded (T) to extended (Y) form. When Gal residues are sialylated the negative charges tend to repel individual branches so that the folded form is preferred in low-ionic-strength solutions. As the ionic strength increases, electrostatic repulsion is gradually shielded and as a result, there is an increase in the extended form and an increase in the apparent size of the

glycoprotein. This explains the dependence of radius of gyration on salts, obtained by Li *et al.* (4).

Biological Significance of Branch Flexibility. The significance of flexible branches in complex carbohydrates remains to be elucidated. Here we discuss the possible roles of flexibility in maintaining glycoprotein structure and in facilitating binding of glycoproteins to lectins.

Complex carbohydrate branch flexibility can function to protect the protein by reducing strains in the linkage between carbohydrate and peptide chain. Modeling has shown that the GlcNAc-Asn linkage is relatively rigid (18). If all branches are maintained in an extended form, collisions with other parts of the molecule and with other molecules may be enough to fracture the glycosidic linkages or cause protein denaturation. In this regard, flexible linkages may act as a shock absorber for the glycoprotein and the flexibility may reduce the total energy of the molecule.

The N-linked oligosaccharides of glycoproteins form a protective barrier against proteolysis. In this regard, the extended branch conformation may actually occupy a smaller surface area whereas the folded conformation may lie along the protein surface, providing greater protection.

The nonreducing terminal residues of complex oligosaccharides are often the recognition determinant that binds to endogenous lectins. Not only is a specific residue(s) recognized (e.g., Gal binding to the asialoglycoprotein receptor) but also the three-dimensional presentation of the target residues is critical as demonstrated for lectin binding of a triantennary glycopeptide (15). The flexible branches of a triantennary glycopeptide might allow a more productive alignment of the trivalent ligand with the three receptor sites. If, for example, Gal-8 were to bind first to the receptor, Gal-6 and -6′ might be able to align faster, due to their attachment to flexible branches, than if simultaneous proper alignment of all three branches were required for binding to occur. The data presented here indicate that at physiological temperature (37°C) virtually all of the branches exist in an extended conformation. However, we cannot discern in this study whether one or more of the branches undergo a conformational change to the folded form upon binding to the receptor. If such a conformational change did occur, it would be accompanied by a release of energy to the system and could perhaps be part of the driving force for binding or lectin internalization. The temperature dependence of the population distribution raises an intriguing question on the "optimal" conformation for binding. Most of the hepatocyte binding studies (e.g., ref. 15) were performed at 0–4°C to avoid internalization. The thermodynamically most favorable conformation was often regarded as the optimal conformation for binding. Obviously, interpretation of the binding data at higher temperature will require additional caution because of our present results.

The large swing of carbohydrate branches due to flexible linkage(s) on protein surface can, in principle, bring two branches on different glycosylation sites very close so that there may be some interactions between glycosylation sites. The swing of one branch at different orientations can cause apparent changes in the molecular weight of a glycoprotein, since the effective size of the carbohydrate is quite large. From the small value of free energy of rotation it is clear that a slight change in solution condition can shift the population of folded or extended form. The conformational heterogeneity may be one of the problems one will encounter in crystallization of glycoproteins. While most manipulation of proteins occurs at low temperature, it appears that to get more uniform carbohydrate structure, one needs to go to higher temperature, which tends to destabilize proteins.

Our previous (13) and present studies show that complex carbohydrates with flexible linkage(s) can adopt different conformations depending on solution conditions. The N-linked oligosaccharides attached to the same glycosylation site in glycoproteins from various sources are generally heterogeneous in structure (14). The structural heterogeneity, together with the conformational heterogeneity, projects extreme complexity to the shape of N-linked oligosaccharides in glycoproteins. It is not clear whether conformational heterogeneity is important in determining structural heterogeneity, but it may contribute to structural heterogeneity since the biosynthesis of complex carbohydrates is a vectorial process and their processing by enzymes depends on physical accessibility (1), which can be altered by changing the orientation of flexible linkage(s).

In this report, we have demonstrated the utility of time-resolved fluorescence energy transfer measurements for studying the solution conformation of a complex oligosaccharide. Especially important is its application at various temperatures, allowing the observation of altered equilibrium states in oligosaccharide conformation. Both the methods and results from this study should be useful in further deciphering the biological roles that complex carbohydrate moieties serve in glycoproteins.

We thank Dr. R. DeToma (Loyola College, Baltimore, MD) for the automation of the instrumentation used here. This work was supported by National Institutes of Health Research Grant DK09970 (Y.C.L.), Grant GM11632 (L.B.), and Postdoctoral Fellowship GM13013-01 Bi-4 (K.G.R.) and by National Science Foundation Grant DIR-8721059 (P.W.). This is publication no. 1473 of the McCollum–Pratt Institute.

1. Kornfeld, R. & Kornfeld, S. (1985) *Annu. Rev. Biochem.* **54**, 631–664.
2. Rademacher, T. W., Parekh, R. B. & Dwek, R. A. (1988) *Annu. Rev. Biochem.* **57**, 785–838.
3. Montreuil, J. (1984) *Pure Appl. Chem.* **56**, 859–877.
4. Li, Z. Q., Perkins, S. J. & Loucheux-Lefebvre, M. H. (1983) *Eur. J. Biochem.* **130**, 275–279.
5. Gervais, M. & Gallot, B. (1982) *Biochim. Biophys. Acta* **688**, 586–596.
6. Davoust, J., Michel, V., Spik, G., Montreuil, J. & Devaux, P. F. (1981) *FEBS Lett.* **125**, 271–276.
7. Homans, S. W., Dwek, R. A. & Rademacher, T. W. (1987) *Biochemistry* **26**, 6571–6578.
8. Cumming, D. A., Shah, R. N., Krepinsky, J. J., Grey, A. A. & Carver, J. P. (1987) *Biochemistry* **26**, 6655–6663.
9. Brockbank, R. L. & Vogel, H. J. (1990) *Biochemistry* **29**, 5574–5583.
10. Imberty, A., Gerber, S., Tran, V. & Perez, S. (1990) *Glycoconjugate* **7**, 27–54.
11. Edge, C. J., Singh, U. C., Bazzo, R., Taylor, G. L., Dwek, R. A. & Rademacher, T. W. (1990) *Biochemistry* **29**, 1971–1974.
12. Haas, E., Wichek, M., Katchalski-Katzir, E. & Steinberg, I. Z. (1975) *Proc. Natl. Acad. Sci. USA* **72**, 1807–1811.
13. Rice, K. G., Wu, P. G., Brand, L. & Lee, Y. C. (1991) *Biochemistry* **30**, 6646–6655.
14. Kobata, A. (1984) in *Biology of Carbohydrates*, eds. Ginsburg, V. & Robbins, P. W. (Wiley, New York), Vol. 2, pp. 87–161.
15. Rice, K. G., Weisz, O., Barthel, T., Lee, R. T. & Lee, Y. C. (1990) *J. Biol. Chem.* **265**, 18429–18434.
16. Rice, K. G. & Lee, Y. C. (1990) *J. Biol. Chem.* **265**, 18423–18428.
17. Badea, M. & Brand, L. (1979) *Methods Enzymol.* **61**, 378–425.
18. Austen, B. M. & Marshall, R. (1974) in *Methodologies de la Structure et du Metabolise des Glycoconjugues*, ed. Montreuil, J. (CNRS, Paris), Centre National de la Recherche Scientifique Colloque no. 221, Vol. 1, pp. 465–482.